

Experimental and ReaxFF-based molecular dynamics studies of the reaction of oxygen with DR-2 as a low global warming potential working fluid

Neng Tao^a, Yuan Cheng^a, Song Lu^a, Haoran Xing^a, Muhammad Usman Shahid^a, Siuming Lo^b, Heping Zhang^{a,*}

^a State Key Laboratory of Fire Science, University of Science of Technology of China, 230026, P.R.China.

^b Department of Civil and Architectural Engineering, City University of Hong Kong, Tat Chee Avenue, Kowloon, Hong Kong

*Corresponding author, Tel: (+86)551 63601665 ; Email address: zhanghp@ustc.edu.cn

Abstract

The cis-1,1,1,4,4,4-hexafluoro-2-butene (DR-2 or HFO-1336mzz(Z)) is a novel environmentally friendly working fluid with appropriate physicochemical characteristics. The present work firstly investigates decomposition mechanism and thermal stability of DR-2 under the atmosphere containing oxygen (O₂) and high temperature experimentally. The oxidative degradation features of DR-2 were explored at the temperature of 473-1073 K and the products were monitored by GC-MS and IC. The experimental and ReaxFF-based molecular dynamics results demonstrated the promotion effects of O₂ on the DR-2 decomposition. The participation of O₂ molecules was supposed to lower the initial thermal decomposition temperature by 240 K approximately and also would increase the number of products such as hydrogen fluoride (HF), but the enhancement effect was weakened by the increasing reaction temperature. The reasonable Arrhenius parameters calculated from the first-order kinetic analyses-based reactive molecular dynamics (RMD) simulations. Combined with density functional theory, the pathways of initial oxidation decomposition product firstly observed in the experimental and RMD simulations were proposed in this study. These results may pave the way for further study of DR-2 as a working fluid with lower global warming potential.

Keywords: ReaxFF MD; DR-2; DFT; oxidation thermal decomposition; HF

29 **1. Introduction**

30 Due to the acceleration of the global warming, hydrocarbons with lower global
31 warming potential (GWP) and zero ozone depletion potential (ODP) are of increasing
32 interest nowadays [1]. As a novel working fluid with low GWP, DR-2, also
33 abbreviated as HFO-1336mzz(Z), is one of the promising alternatives for HFC-245fa
34 in the organic Rankine cycle (ORC) systems [2] and R134a in the Ejector Cooling
35 Cycle systems [3]. In comparison with the first commercially available
36 hydrofluoroolefins (HFOs) such as HFO-1234yf and HFO-1234ze-E, DR-2 shows the
37 features of non-flammability at both 333 K and 373 K and chemical stability at high
38 temperatures [4]. Moreover, DR-2 exhibited superior thermal properties to
39 HCFO-1233zd (E) in the systems of ORC and vapor compression cycle [5]. Both the
40 environmental friendliness and the extremely low acute toxicity of DR-2 will not
41 cause irritation to human skin and eyes [6].

42 Previous studies mainly focused on the thermal stability, thermal decomposition
43 mechanism and basic physical and chemical parameters of DR-2, and very
44 meaningful results were obtained through experiments and theoretical calculations.
45 Tao et al. [7] evaluated the production of hydrogen fluoride (HF) of pure DR-2 at
46 873–1073 K in experiments. Huo et al. [8] studied the effect of pressure (2.1, 3.1 and
47 4.0 MPa) on DR-2 for 24h, and the dissociation temperature was 583 K to 603 K, 563
48 K to 583 K, and 543 K to 563 K, respectively. Huo et al. [9] investigated the pyrolysis
49 process and product of DR-2 at 2000-3000 K with ReaxFF simulations, and the DR-2
50 decomposition was divided into three phases. The same research group also discussed
51 the impacts of copper (Cu), oxygen (O₂), water (H₂O) and polyol ester (POE)
52 lubricants on the decomposition of DR-2 [10-13]. Except for a working fluid, DR-2
53 was considered to be a promising fire extinguishing alternative for halon [14, 15].

54 The ReaxFF reaction force field was used to explore the complicated phenomena
55 containing bond formation and breakage [16]. Therefore, the pyrolysis and oxidation
56 decomposition of working fluids was extensively studied with ReaxFF simulation [11,

12, 17]. Moreover, the density functional theory (DFT) calculation was frequently conducted to investigate the chemical reactions of organic working fluids. Wang [18] et al. explored the further reaction of DR-2 products with active radicals such as OH· and H· radicals by DFT. Zhang [19] et al. reported the decomposition mechanism by DFT for the first time by studying the main pathways of the $\text{CF}_3\text{CF}=\text{CH}_2$ decomposition. Huang[20] et al. investigated the formation mechanisms of the main products (CO, CO_2 and CH_4) in the thermal decomposition of lignin.

The heat sources are usually divided into both high-temperature and low-temperature heat sources according to different temperature ranges [1]. The working temperature of high-temperature heat sources can reach 873 K. At a higher operating temperature, the organic working fluid used in a supercritical ORC could be thermally decomposed, resulting in the changes in the thermal characteristics of the working fluid and the deviation of the parameters from the design conditions. The non-condensable gases and polymers produced from the thermal decomposition may cause the deterioration of heat transfer and blockage of the pipeline, which could lead to the safety problems in the ORC system. DR-2 was used as a working fluid with lower GWP in the ORC system for the experimental evaluation of micro-scale cryogenic applications[21]. Thus, it is of great importance to study its thermal decomposition features under high temperature and oxygen-containing conditions. Although the physicochemical properties of DR-2 have been extensively reported, its thermal decomposition products in the presence of O_2 at high temperatures are still unclear.

In this study, we investigate the initial decomposition temperature, main product such as HF and the related kinetics of DR-2 in the presence of O_2 experimentally and RMD simulations under high temperature. It is expected to benefit the environment protection and the industry application security of DR-2.

2. Methodologies

2.1 Experimental apparatus and procedures

In the experimental system (Fig 1), the pyrolysis process of DR-2 was studied in the atmospheres of two gases (pure N₂ and synthetic air) from 473 to 1073 K. The CF₃CH=CHCF₃ with a purity of above 99.5% (Kemu Fluoride Technology Co., Ltd.) was used directly without purification. The nitrogen with a purity of above 99.99% and the synthetic air with a composition of 21% O₂ and 79% N₂ employed in the experiments were provided by the local commercial suppliers. Prior to the thermal degradation experiment, the preheating of each quartz tube was conducted at 1123 K under argon flow for 1 h. The argon gas (purity $\geq 99.99\%$) was used to purge the impurity gases in the experimental pipeline. The gasification of pure DR-2(l) was realized by preheating it to 343 K. At the same time, the reactor temperature was set to 473-1073 K with a constant temperature zone length of 225 mm (± 5 K). The quartz tube in the tube furnace could be replaced with a new one at a varying decomposition temperature. The length and inner diameter of the quartz tubular reactor were 1100 mm and 10 mm, respectively. In the experiment, the temperature of the furnace was set to 473-973 K with an interval of 100 K and 973-1073 K with an interval of 20 K, respectively. After the temperature was kept at the above-mentioned set points for 2 h, the vaporization setup was heated with a peristaltic pump flow rate of 0.41 mL/min and a mass flowmeter value of 100 mL/min. The pyrolysis time was 0.5 h. The thermal degradation products of DR-2 were collected by the gas-collecting pockets and 400 mL of deionized water. Finally, the exhaust gases at the end of the experiment were disposed by sodium hydroxide (NaOH) aqueous solution before discharge. The fluoride concentration in the solution was measured by the ion chromatography (IC) after the adsorption of gas products in 400 mL of deionized water. Finally, the exhaust gases were analyzed by GC-MS.

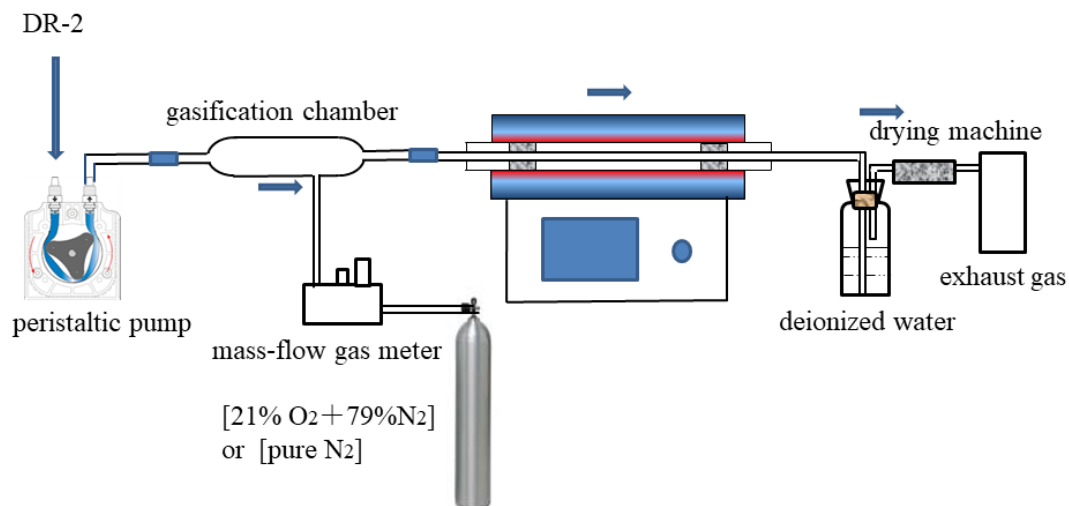


Fig 1. Scheme of the DR-2 oxidation pyrolysis system.

2.2 ReaxFF MD simulations

Although part of the thermal decomposition products was detected in the thermal decomposition experiment, the intermediate products and the product formation mechanism are still unknown. The quantum chemistry calculation by the simulation method of ReaxFF-MD could be in good consistence with corresponding experimental results. This method was widely used in various reaction systems, such as the thermal decomposition of fossil fuels, the oxidation or combustion processes of alkanes and hydrocarbons, and the explosion of energetic materials [17, 22-24]. The bond formation and breakage in the molecular dynamic simulation could be described by ReaxFF, a reactive force field based on the bond order firstly proposed by van Duin [25, 26].

The ReaxFF energy function was expressed by Equation (1).

$$E_{system} = E_{bond} + E_{over} + E_{under} + E_{val} + E_{pen} + E_{tors} + E_{conj} + E_{vdWaals} + E_{Coulomb} \quad (1)$$

Where E_{bond} is the bond energy, E_{over} is the over-coordinated atom in the molecular energy contribution (MEC), E_{under} is the under-coordinated atom in the MEC, E_{val} is the valence angle terms, E_{pen} is the penalty energy, E_{tors} is the

torsion energy, E_{conj} is the conjugation effects in the energy contribution, $E_{vdWaals}$ is the non-bonded van der Waals interactions, and $E_{Coulomb}$ is the non-bonded Coulomb interactions.

In order to accelerate the reaction speed within the simulation time range, the simulation temperature range was set to 1000-3400 K (higher than experimental temperature in this work) to study the pyrolysis mechanism of DR-2. In a reasonable time, the simulated temperature should be higher than the actual temperature in average to speed up the dynamic simulation of the activation process [27, 28]. According to Arrhenius equation [29], temperature will only change the reaction rate to a certain extent, but will not change the reaction path.

2.3 Density functional theory (DFT) calculations

To investigate the initiation mechanism of DR-2 oxidation and dissociation, the DFT approach was used to compute the initial reaction energy barriers based on the products of the experimental results. By the B3LYP method, based on 6-311 ++ G (d, p), the reactant geometric structure, the transition state and the initial decomposition pathway were optimized at 298 K and 0.1 MPa. The Gaussian 09 suite of programs was employed for the calculation of all the reactions [30].

3. Results and discussion

3.1 Experimental Section

3.1.1 The Trend of Hydrogen Fluoride Concentration

Due to the toxicity of HF, it is noteworthy of monitoring the content variation of HF generated during the DR-2 decomposition. The gradual increases in the hydrogen ion concentration ($[H^+]$) and the fluoride ion concentration ($[F^-]$) were accompanied by the increasing pyrolysis temperature (473-1033 K), and the tendency of increase was finally stabilized (Fig. 2). Under different gas atmospheres, drastic changes in $[H^+]$

and $[F^-]$ were observed at varying temperatures. In the pure nitrogen atmosphere, great changes in the pH and $[F^-]$ of the solution were seen due to the absorption of the thermal decomposition products at 1013 K. However, in the atmosphere of synthetic air, the sharp concentration variations were found at 773 K. Obviously, the amount of HF produced in synthetic air was higher than that in pure N_2 . Thus, the presence of O_2 would facilitate the DR-2 decomposition. On the one hand, O_2 would lower the degradation temperature of DR-2 from 1013 K to 773 K. On the other hand, the increased HF content generated under oxygen-containing conditions would enhance the thermal decomposition degree of DR-2. When the temperature reached a certain level, the decomposition rate of DR-2 would quickly change, but the effect of increasing the temperature on thermal decomposition would weaken or disappear. It is easy to find that the pH value remains unchanged when a certain temperature is reached, but the fluoride ion concentration ($[F^-]$) continues to increase, because the deionized water also absorbs other fluorine-containing products. This would result in a lower concentration of HF released from the experiment, since the silicon tetrafluoride was detected on the surface of the reaction quartz tube.

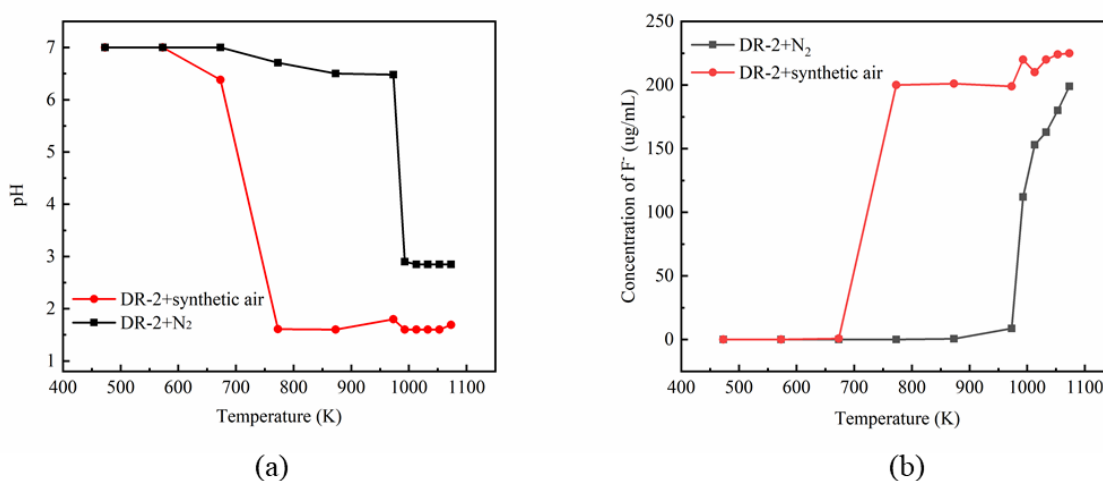


Fig 2. The change of pH and $[F^-]$ formed in the DR-2 decomposition at different temperatures.

3.1.2 GC-MS analyses of the gaseous products

The gaseous products generated by the oxidation thermal decomposition were

collected in the solution. The DR-2 oxidation products were identified by the GC-MS method. Two main peaks were seen in the GS-MS analysis (Fig. 3), indicating the undecomposed synthetic air and DR-2 in the collected gases. Upon higher thermal decomposition temperature, a small peak in Fig. 3 (b) was observed, which was identified as $C_4H_2OF_6$ based on the standard mass spectrum library.

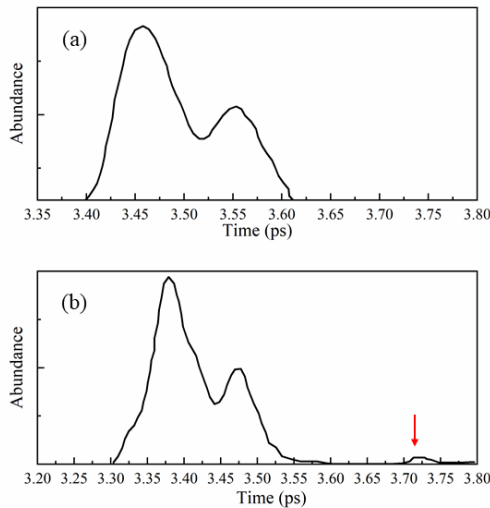


Fig 3. GC–MS results of the exhaust gas of DR-2 oxidation Pyrolysis
(a: 673 K; b: 1103 K)

3.2 ReaxFF-MD simulation

To simulate the actual conditions, the initial densities of the system containing DR-2 and O_2 were set as 1.36 g cm^{-3} (the actual liquid density at 300 K and 0.1 MPa) and $0.00538 \text{ g cm}^{-3}$ (the actual vapor density at 300 K and 0.1 MPa) [5]. Therefore, the initial densities of the system containing DR-2 set in this work were of great importance. Such densities in previous work was 1.3595 and 0.015 g cm^{-3} (Table 1).

Table 1

Initial densities and ensemble of ReaxFF simulation about DR-2.

	Molecules	Initial density ($\rho/\text{g} \cdot \text{cm}^{-3}$)	Ensemble
Ref.[9]	50 DR-2	1.3595	NVT
Ref.[11]	150 DR-2 + 450 O_2 (1)	0.015 (1)	NVT
	75 DR-2 + 450 O_2 (2)		
	300 DR-2 + 450 O_2 (3)		

Ref.[12]	150 DR-2 + 450 O ₂ (1)	0.015	NVT
	150 DR-2 + 450 O ₂ + 37 H ₂ O (2)		
	150 DR-2 + 450 O ₂ + 75 H ₂ O (3)		
	150 DR-2 + 450 O ₂ + 112 H ₂ O (4)		
	150 DR-2 + 450 O ₂ + 150 H ₂ O (5)		
This work	100 DR-2 + 50 O ₂ (1)	0.00538 (1)	NVT
	45 DR-2 (2)		
	45 DR-2 + 5 O ₂ (3)	1.36 (2-3)	

To understand the pyrolysis process induced by the temperature, the RMD simulations at varying temperatures were carried out on the pure DR-2 system and the system including DR-2 and O₂ for the first time. The pure 45 DR-2 or 45 DR-2 and 5 O₂ were placed in two periodic boxes measuring 20.81 Å × 20.81 Å × 20.81 Å (Φ_1) and 20.96 Å × 20.96 Å × 20.96 Å (Φ_2) with a system density of 1.36 g · cm⁻³ (Fig. 4). The system Φ_1 and Φ_2 were first minimized via MD at a low temperature (5 K) with the NVT ensemble and then were equilibrated with the NVT ensemble for 50 ps at 300 K using a time step of 0.1 fs. The temperature was elevated from 1000 K to 3400 K with a ramp of 9.6 K · ps⁻¹ for 250 ps, followed by maintaining for 50 ps at 3400 K.

To study the kinetic analysis of the pure DR-2 and the system containing DR-2 and O₂ at elevated temperatures, the RMD simulations were employed with NVT (constant particle number, constant volume, and constant temperature) ensemble at 2600-3400 K with an interval of 200 K and a reaction time of 100 ps. Prior to the desired RMD simulations, the systems Φ_1 and Φ_2 were equilibrated for 50 ps (picosecond) at 300 K.

To study the pyrolysis product distribution of the system including DR-2 and O₂, the oxidation decomposition process was analyzed by the RMD simulations. The 100 DR-2 and 50 O₂ were placed in unit cells and the molecules structure were optimized (Fig. 4). The sides of unit cells were 177.11 Å × 177.11 Å × 177.11 Å (Φ_3) with a density of 0.00538 g · cm⁻³.

For all the ReaxFF simulations, the ReaxFF parameters [31] for C, H, O and F atoms were adopted in this work. Recent studies [11, 12] used in this ReaxFF

parameters have revealed that the outcomes at high temperatures of ReaxFF MD simulations on DR-2 were in good agreement with those of experiments [14, 18]. And the reaction temperature was adjusted by a Berendsen thermostat with a damping constant of 200 fs.

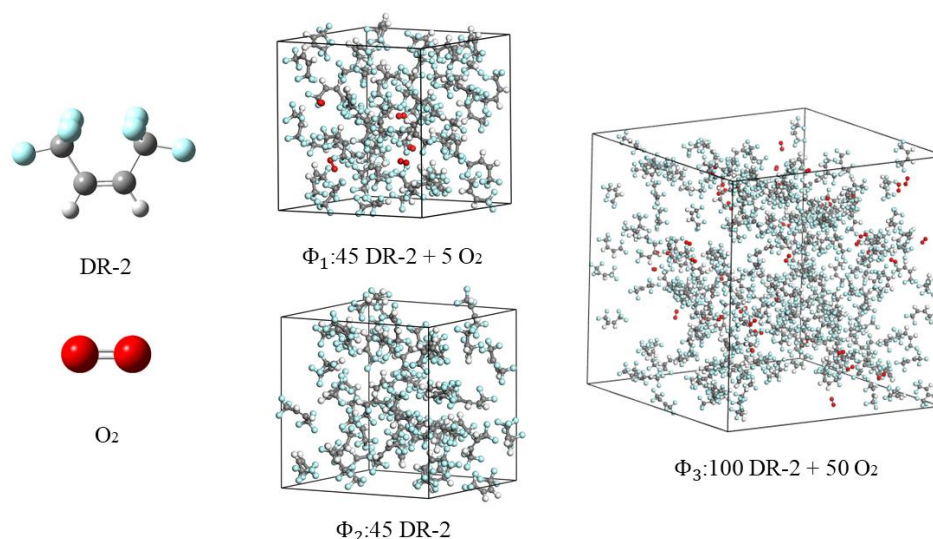


Fig 4. The snapshots of optimized molecular structure and the equilibrated unit cells of the DR-2 with O₂ (The colors of gray, white, red, and blue spheres represented the C, H, O, and F atoms, respectively.)

3.2.1 Initial decomposition temperature and kinetic analysis of DR-2 (liquid) decomposition in the absence and presence of O₂

To obtain the initial decomposition temperature of DR-2 (liquid), the RMD simulations in the absence and presence of O₂ were conducted at the temperature of 1000-3400 K and a density of 1.36 g·cm⁻³. Clearly, the initial dissociation temperature of pure DR-2 was about 2713 K at 178 ps (Fig. 5(a)), and the DR-2 in the presence of O₂ began to decompose at 2484 K and a time of 178 ps (Fig. 5(b)) approximately. The initial degradation temperature of DR-2 was reduced from 2723 K to 2484 K in the presence of O₂ molecules. It also can be found that DR-2 and O₂ molecules start to dissociate almost simultaneously. When the temperature reaches

230 3400 K, the reactant molecules would be consumed completely

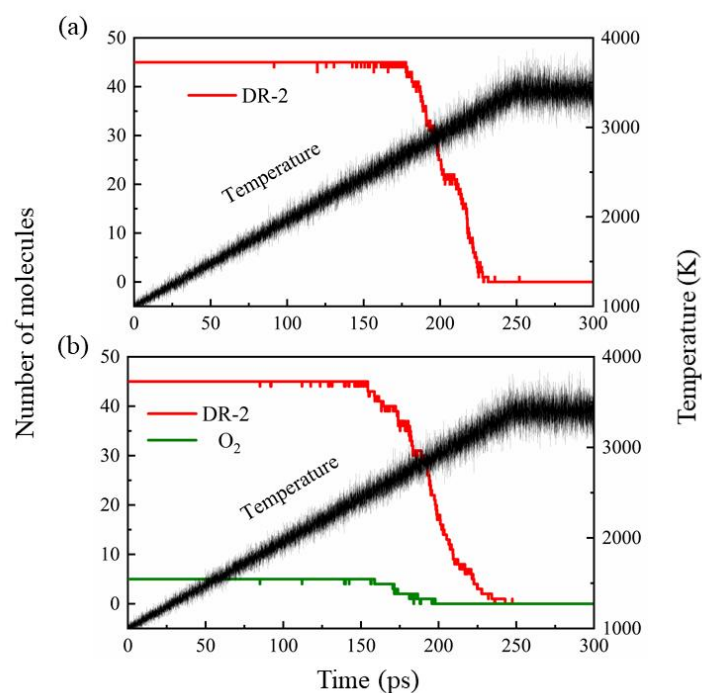


Fig 5. The time evolutions of the DR-2 (a) in the absence and (b) presence of O₂ at a density of 1.36 g·cm⁻³ and a temperature of 2600-3400K in RMD simulation

According to the consumption rate and the initial decomposition temperature of DR-2 in Fig. 5, the temperature-dependent NVT-MD simulations were carried out for kinetic analysis of the DR-2 degradation in the absence and presence of O₂ at 100 ps and a temperature of 2600-3400 K with an interval of 200 K. The increasing temperature was accompanied by the obvious increase of decomposition rates of DR-2 (Fig. 6). In addition, the dissociation of DR-2 was especially accelerated by 5 O₂ molecules at lower temperatures of 2600 K and 2800 K, and this impact became insignificant at the temperature higher than 3000 K. Because the high energy self-dissociation pathway became accessible for DR-2 when the temperature up to 3000K. At the same time, the presence of O₂ molecules became insignificant at higher temperature.

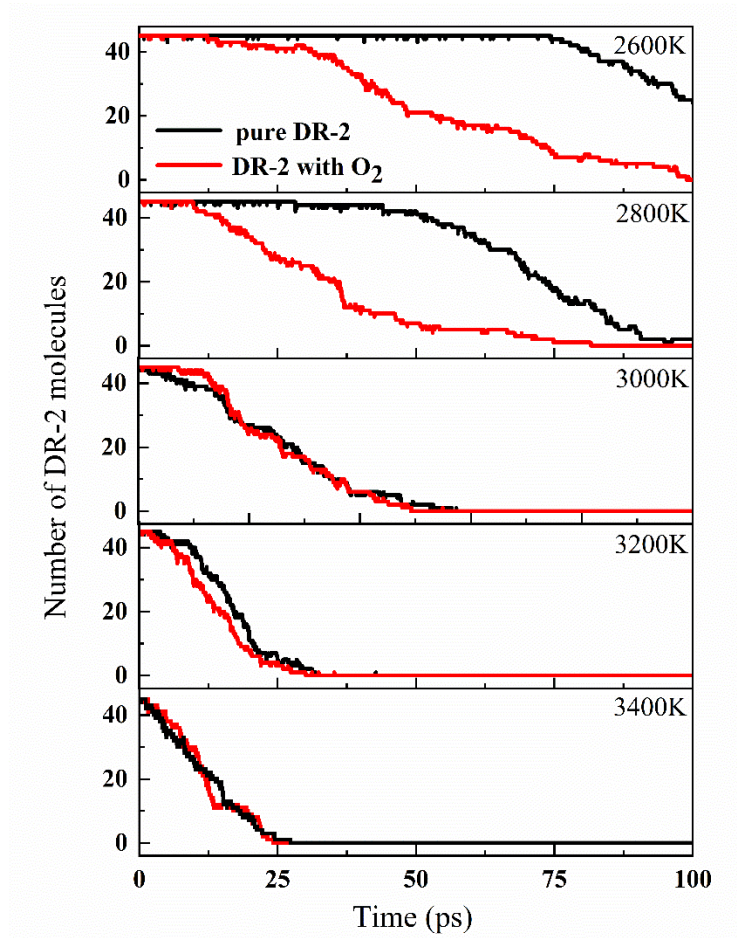


Fig 6. Comparison of time evolutions of DR-2 in the absence and presence O₂ in NVT-MD simulation at a density of 1.36 g·cm⁻³ at 2600K, 2800K, 3000K, 3200K and 3400K, respectively.

The rate constant k at each temperature was calculated by the relation of the number of DR-2 molecules over time through first-order kinetics:

$$\ln N_t - \ln N_0 = -kt \quad (2)$$

where N_0 and N_t are the number of DR-2 molecules at the beginning and at time t , respectively.

$$\ln k = \ln A - E_a/Rt \quad (3)$$

where R is the universal gas constant and T is the pyrolysis temperature. The fitted Arrhenius plot of the DR-2 decomposition process in the absence and presence of O₂ were shown in Fig. 7. The activation energy (E_a) of thermal decomposition of DR-2 in the presence of O₂ was calculated to be about 191.9 kJ/mol, being about 100 kJ/mol lower than that for pure DR-2.

Based on the effect of O₂ molecules on the initial decomposition temperature and

kinetics during the DR-2 degradation, the DR-2 decomposition could be strongly promoted by a small amount of O₂ molecules at high temperatures in a liquid state. Thus, it was of great significance to exclude O₂ or air when DR-2 was acted as a high-temperature working fluid. However, there is no experimental data on liquid DR-2 decomposition with O₂ currently and the relevant experiments are needed to compare with the theoretical results in this work for future research.

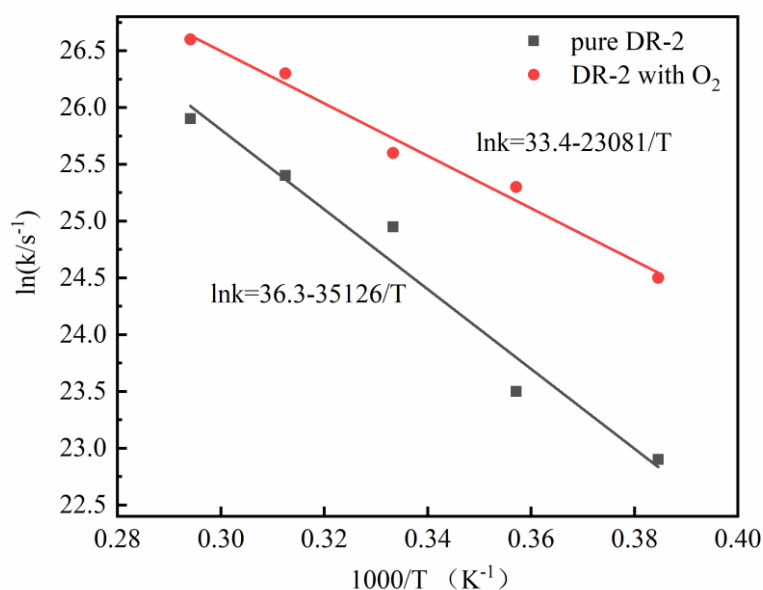


Fig 7. The fitted rate constant versus temperature (2600-3400 K) obtained from 100 ps NVT-RMD simulations at a density of 1.36 g·cm⁻³ of DR-2 pyrolysis in the absence and presence of O₂.

3.2.2 Temperature effects on DR-2 (vaporous) decomposition in presence of O₂

By considering the amounts of synthetic air and DR-2 in our experiment and the vapor density of DR-2 (0.00538 g cm⁻³) at 300 K and 0.1 Mpa, a series of ReaxFF simulations were conducted with NVT ensemble at 2600 K, 2800 K, 3000 K, 3200 K and 3400 K and a reaction time of 500 ps to obtain the oxidation process and products of DR-2.

The oxidation dissociation process of Φ_3 for 500 ps at 3400 K was investigated (Fig. 8). Clearly, HF and CO were the main products of thermal

decomposition of DR-2. The thermal degradation process of the system could be divided into 3 phases. In the first stage (0-175 ps), the consumption of oxygen molecules was relatively low, and DR-2 molecules underwent self-thermal decomposition to produce radicals. In the second phase (175-325 ps), the number of O_2 was equal to that of DR-2 molecules at the beginning. The collision of radicals and O_2 molecules with DR-2 resulted in the decomposition and final consumption of DR-2 together with O_2 . The number of CF_3 radicals was increased up to the maximum value, followed by the slow consumption. The reaction of O_2 with DR-2 molecules was accompanied by the breakage of the C-F bond and the production of more F radicals. The CO molecules and O radicals reached their maximum values at this stage as the thermal decomposition continued. In the third stage (325-500 ps), the numbers of HF and F were increased to the maximum.

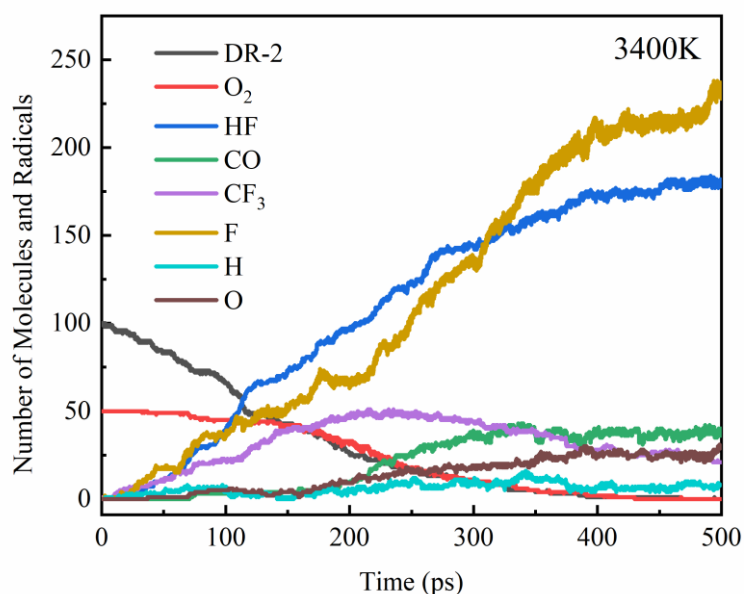


Fig 8. The oxidation decomposition of DR-2 at 3400K

In RMD simulations and experiments, HF was obviously the main product of the oxidative decomposition reaction of DR-2. The evolution of the number of HF at 2600-3400 K over the time in the ReaxFF simulations was studied (Fig. 9). The increasing temperature was accompanied by the obviously increasing amount of HF.

At 3000 K, the number of HF molecules was increased by 2-3 times. This phenomenon was consistent with previous experiment. At the temperature of 2600 K, the production of HF occurred at around 300 ps and reached around 40 at 500 ps. At the temperature of 2800 K, the time for the production of HF was advanced, and finally the production reached about 60. At 3000-3400 K, the HF generation rate was significantly improved, and the final HF amount was 150-200. At this time, the increase in temperature demonstrated a small effect on the production of HF. This was consistent with the experimental results.

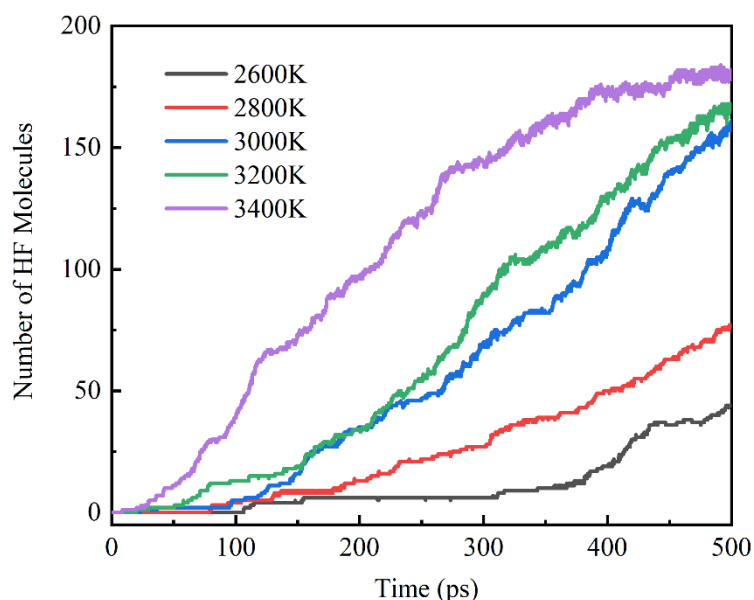


Fig 9. The evolution of the HF production at different temperatures over time

As detected to be the principal product by GC-MS in Section 3.1, $\text{CF}_3\text{CHOCHCF}_3$ was also found in the ReaxFF-MD simulation at 2600-3400 K (Fig. 10). At 2600 K, the production of $\text{CF}_3\text{CHOCHCF}_3$ molecule occurred at 350-500 ps and the number of the molecule was just one. At 2800-3400 K, the production of $\text{CF}_3\text{CHOCHCF}_3$ molecule occurred at 50-150 ps and the number of this molecule was just 1-10. Thus, the $\text{CF}_3\text{CHOCHCF}_3$ molecule was an intermediate and its residence time in the system was relatively short.

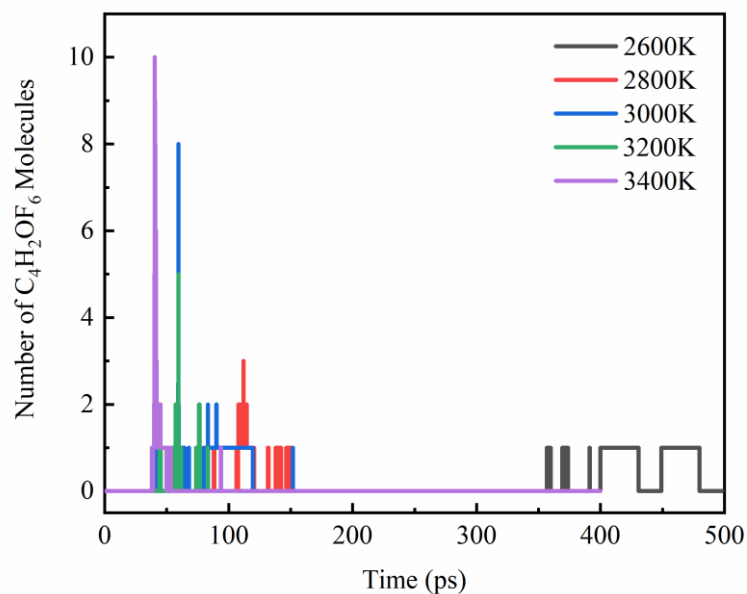


Fig 10. The evolution of the number of $C_4H_2OF_6$ molecule at different temperatures over time

The radicals were generated during the collision reaction between O_2 and DR-2 and the DR-2 self-decomposition, thereby promoting the completion of the reaction. The evolution of the number of small radicals containing F, CF_3 , H and O radicals at different temperatures over time was shown in Fig. 11. The constant increase of the F radical number was accompanied by the rising temperature. At lower temperatures of 2600 K and 2800 K, the continuous increase in CF_3 radicals and F radicals was observed over time, and the final production amounts were equivalent. However, at 3000-3400 K, the increase in the number of CF_3 radicals was followed by a decrease, and the time to reach the maximum was continuously shortened. The numbers of O and H radicals were less in the whole reaction.

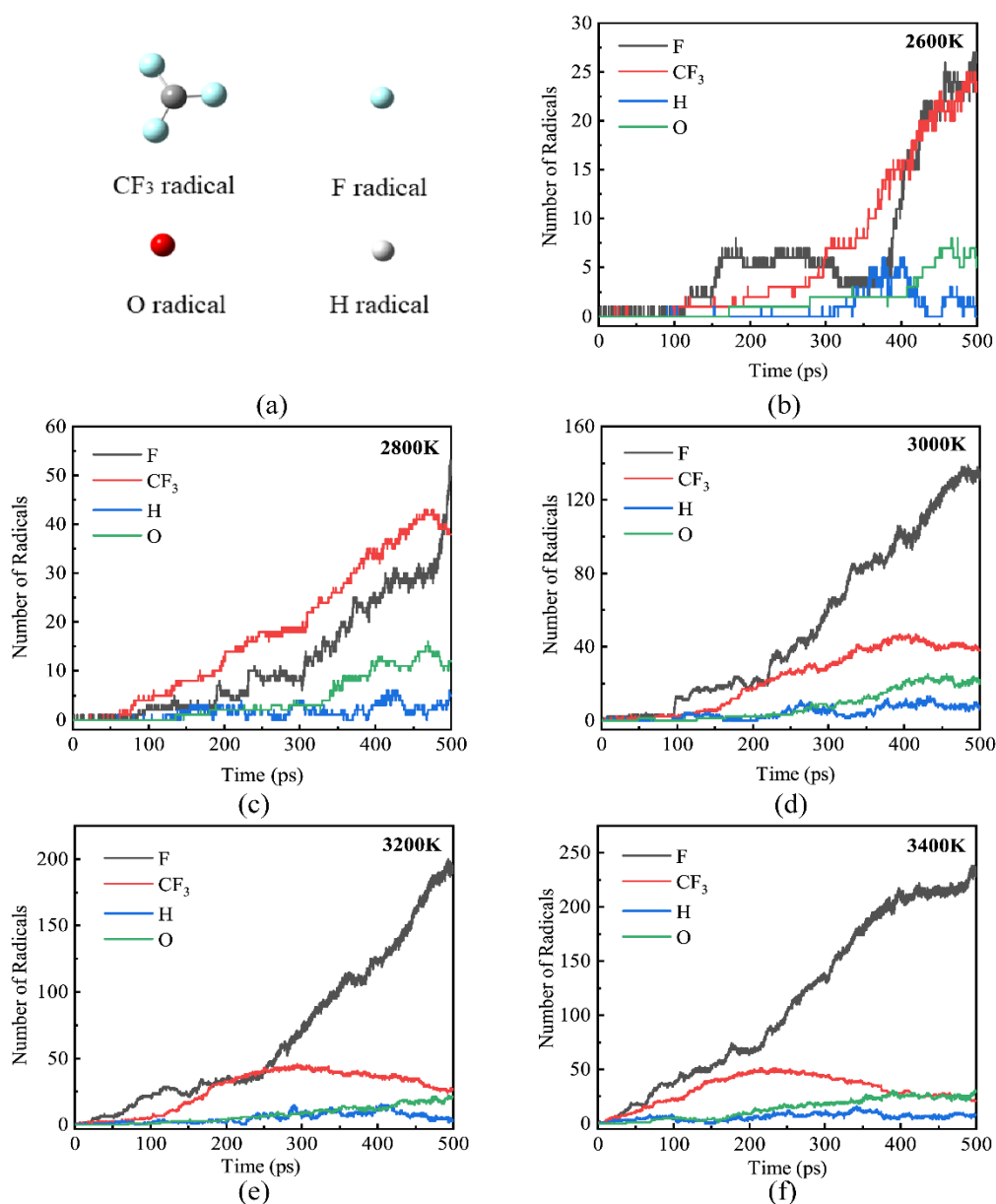


Fig 11. The evolution of the number of small radicals at different temperatures over time (The colors of gray, white, red, and blue spheres represented the C, H, O, and F atoms, respectively.)

3.3 Initiation oxidation decomposition reactions of DR-2

In both the experimental and the ReaxFF simulation parts, extremely lower content of CF₃CHOCHCF₃ was found than HF, indicating that it may be an intermediate product of the oxidation thermal decomposition of DR-2. The DFT approach was used to compute the formation process and energy barrier of

CF₃CHOCHCF₃. The O₂ molecules attacked C atoms in C=C bonds, forming TS1
 with an energy barrier of 127.1 kJ/mol (Fig. 12). This energy barrier was lower than
 the bond dissociation energy of DR-2, so the O₂ molecule could promote the
 decomposition of DR-2 at high temperatures. As described in the ReaxFF simulation,
 the self-oxidative decomposition of DR-2 may generate CF₃, F, H and O radicals. For
 example, the H radical oxidative thermal decomposition system would react with
 TS1-pro and form TS2-pro (OH radical and CF₃CHOCHCF₃) and release 124.3
 kJ/mol, implying the promotion effect of H radical on the progress of the reaction (Fig.
 13). Meanwhile, the CF₃, F and O radicals also would react with TS1-pro to form
 CF₃CHOCHCF₃.

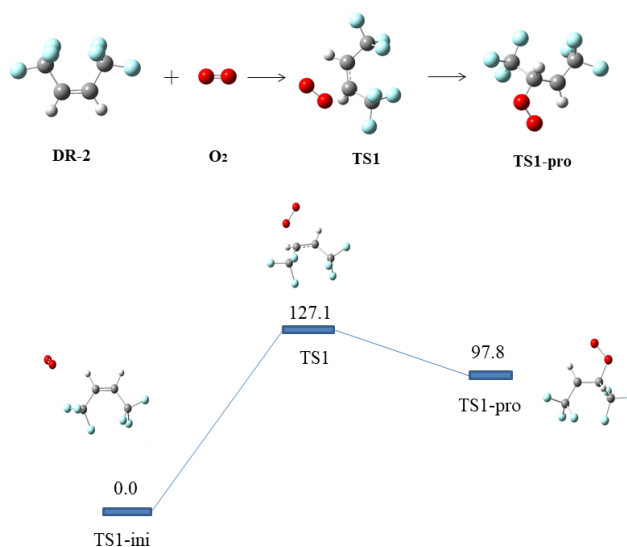


Fig 12. The proposed pathways and energy profiles of the collision of between oxygen and DR-2
 (The colors of gray, white, red, and blue spheres represented the atoms of C, H, O, and F,
 respectively.)

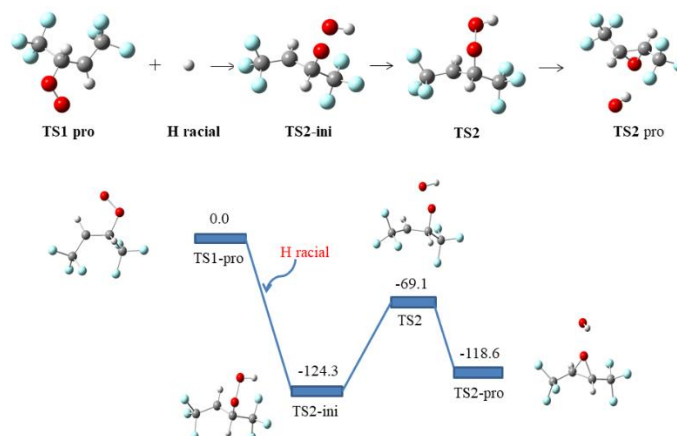


Fig 13. The proposed pathways and energy profiles of DR-2 and H radical
(The colors of gray, white, red, and blue spheres represented the atoms of C, H, O, and F,
respectively.)

4. Conclusion

The oxidation thermal decomposition of DR-2 was investigated experimentally and theoretically at high temperature in this study. The experimental investigated main DR-2 decomposition products under high temperature (from 473K to 1073K) in a tubular reactor detected by IC and GC-MS. A series of the reactive molecule dynamics (RMD) simulations were conducted to figure out the effect of O₂ molecules on the decomposition of DR-2 at liquid and vaporous state. The possible pathways of the initial decomposition products of C₄H₂OF₆ were proposed by DFT method. The conclusions can be summarized as follows:

(1) The promoting effect of O₂ molecules on DR-2 was manifested in two aspects. The thermal decomposition degree and decomposition products such as HF increased by lowering the initial thermal decomposition temperature of DR-2 (from 993 K to 673 K). However, this promoting effect would be weakened when a certain temperature was reached.

(2) HF was one of the main products of thermal decomposition of DR-2 with O₂ under high temperature, and the ReaxFF MD simulation were in good agreement with the experimental results.

(3) The activation energy (E_a) of thermal decomposition of DR-2 in the presence of O₂ was calculated from RMD simulations based on kinetic analysis to be about 191.9 kJ/mol, being 100 kJ/mol lower than that for pure DR-2 approximately.

(4) Both the GC-MS and ReaxFF MD simulation results detected the oxidation product of the double bond in DR-2, and the process of O₂ molecule attacking DR-2 to form the oxidation products was deduced in combination with the DFT method.

378 **Acknowledgments**

379 The quantum chemical calculations were conducted through ADF software and
380 the supercomputing system at State Key Laboratory of Fire Science of USTC.

381

382

383

384

385

386

387

388

389

390

391

392

393

394

395

396

397

398

399

400

401

402

403

404 **References**

- 405 1. Moles, F., et al., *Thermo-economic evaluation of low global warming potential*
406 *alternatives to HFC-245fa in Organic Rankine Cycles*. Energy Procedia, 2017.
407 **142**: p. 1199-205.
- 408 2. Moles, F., et al., *Thermo-economic evaluation of low global warming potential*
409 *alternatives to HFC-245fa in Organic Rankine Cycles*, in *Proceedings of the 9th*
410 *International Conference on Applied Energy*, J. Yan, J. Wu, and H. Li, Editors.
411 2017. p. 1199-1205.
- 412 3. Gil, B. and J. Kasperski, *Efficiency Evaluation of the Ejector Cooling Cycle*
413 *using a New Generation of HFO/HCFO Refrigerant as a R134a Replacement*.
414 Energies, 2018. **11**(8).
- 415 4. Kontomaris, K., *HFO-1336mzz-Z: High Temperature Chemical Stability and*
416 *Use as A Working Fluid in Organic Rankine Cycles*. International Refrigeration
417 and Air Conditioning Conference, 2014b: p. 1525.
- 418 5. Moles, F., et al., *Low GWP alternatives to HFC-245fa in Organic Rankine*
419 *Cycles for low temperature heat recovery: HCFO-1233zd-E and*
420 *HFO-1336mzz-Z*. Applied Thermal Engineering, 2014. **71**(1): p. 204-212.
- 421 6. *Cis-1,1,1,4,4,4-hexafluoro-2-butene (HFO-1336mzz-Z) (2018)*. Toxicology and
422 industrial health, 2019: p. 748233719825530.
- 423 7. Tao, N., et al., *Experimental and Density Functional Theory Studies on*
424 *1,1,1,4,4,4-Hexafluoro-2-Butene Pyrolysis*. Molecules (Basel, Switzerland),
425 2020. **25**(17).
- 426 8. Huo, E.G., et al., *Thermal stability and decomposition mechanism of*
427 *HFO-1336mzz(Z) as an environmental friendly working fluid: Experimental*
428 *and theoretical study*. International Journal of Energy Research, 2019. **43**(9): p.
429 4630-4643.
- 430 9. Huo, E.G., et al., *A ReaxFF-based molecular dynamics study of the pyrolysis*
431 *mechanism of HFO-1336mzz(Z)*. International Journal of Refrigeration-Revue
432 Internationale Du Froid, 2017. **83**: p. 118-130.
- 433 10. Huo, E., et al., *Dissociation mechanisms of HFO-1336mzz(Z) on Cu(111),*
434 *Cu(110) and Cu(100) surfaces: A density functional theory study*. Applied
435 Surface Science, 2018. **443**: p. 389-400.
- 436 11. Huo, E., et al., *A ReaxFF-based molecular dynamics study of the oxidation*
437 *decomposition mechanism of HFO-1336mzz(Z)*. International Journal of
438 Refrigeration-Revue Internationale Du Froid, 2018. **93**: p. 249-258.
- 439 12. Huo, E.G., et al., *The oxidation decomposition mechanisms of HFO-1336mzz(Z)*
440 *as an environmentally friendly refrigerant in O-2/H2O environment*. Energy,
441 2019. **185**: p. 1154-1162.
- 442 13. Huo, E., et al., *Experimental and theoretical studies on the thermal stability and*
443 *decomposition mechanism of HFO-1336mzz(Z) with POE lubricant*. Journal of
444 Analytical and Applied Pyrolysis, 2020. **147**.
- 445 14. Wang, Y., et al., *Theoretical and experimental studies on the thermal*

- decomposition and fire-extinguishing performance of
cis-1,1,1,4,4,4-hexafluoro-2-butene. International Journal of Quantum
 Chemistry, 2020. **120**(9).
15. Zhang, H., et al., *Thermal Decomposition Mechanism and Fire-Extinguishing Performance of trans-1,1,1,4,4,4-Hexafluoro-2-butene: A Potential Candidate for Halon Substitutes*. Journal of Physical Chemistry A, 2020. **124**(28): p. 5944-5953.
 16. Xin, L., et al., *Thermal decomposition mechanism of some hydrocarbons by ReaxFF-based molecular dynamics and density functional theory study*. Fuel, 2020. **275**.
 17. Cao, Y., et al., *Influence of water on HFO-1234yf oxidation pyrolysis via ReaxFF molecular dynamics simulation*. Molecular Physics, 2019. **117**(13): p. 1768-1780.
 18. Wang, X., et al., *Suppression of propane cup-burner flame with HFO-1336mzz(Z) and its thermal stability study*. Thermochemica Acta, 2020. **683**.
 19. Zhang, H., et al., *Mechanism of thermal decomposition of HFO-1234yf by DFT study*. International Journal of Refrigeration-Revue Internationale Du Froid, 2017. **74**: p. 399-411.
 20. Huang, J., et al., *A density functional theory study on formation mechanism of CO, CO₂ and CH₄ in pyrolysis of lignin*. Computational and Theoretical Chemistry, 2014. **1045**: p. 1-9.
 21. Navarro-Esbri, J., et al., *Experimental study of an Organic Rankine Cycle with HFO-1336mzz-Z as a low global warming potential working fluid for micro-scale low temperature applications*. Energy, 2017. **133**: p. 79-89.
 22. Zheng, M., et al., *Initial Chemical Reaction Simulation of Coal Pyrolysis via ReaxFF Molecular Dynamics*. Energy & Fuels, 2013. **27**(6): p. 2942-2951.
 23. Beste, A., *ReaxFF Study of the Oxidation of Softwood Lignin in View of Carbon Fiber Production*. Energy & Fuels, 2014. **28**(11): p. 7007-7013.
 24. Ren, C., et al., *Decomposition mechanism scenarios of CL-20 co-crystals revealed by ReaxFF molecular dynamics: similarities and differences*. Phys Chem Chem Phys, 2020. **22**(5): p. 2827-2840.
 25. van Duin, A.C.T., et al., *ReaxFF: A reactive force field for hydrocarbons*. Journal of Physical Chemistry A, 2001. **105**(41): p. 9396-9409.
 26. Chenoweth, K., A.C.T. van Duin, and W.A. Goddard, III, *ReaxFF reactive force field for molecular dynamics simulations of hydrocarbon oxidation*. Journal of Physical Chemistry A, 2008. **112**(5): p. 1040-1053.
 27. Ashraf, C., et al., *Pyrolysis of binary fuel mixtures at supercritical conditions: A ReaxFF molecular dynamics study*. Fuel, 2019. **235**: p. 194-207.
 28. Sorensen, M.R. and A.F. Voter, *Temperature-accelerated dynamics for simulation of infrequent events*. Journal of Chemical Physics, 2000. **112**(21): p. 9599-9606.

- 488 29. Cao, Y., et al., *Thermal decomposition of HFO-1234yf through ReaxFF*
489 *molecular dynamics simulation*. Applied Thermal Engineering, 2017. **126**: p.
490 330-338.
- 491 30. Gaussian., R.A., Frisch, G.W.T.M.J., Schlegel, H.B., Scuseria, G.E., Robb,
492 J.R.C.M.A., Scalmani, G., Barone, V. Mennucci, B., Petersson, H.N.G.A.,
493 Caricato, M., Li, X., Hratchian, H.P., Izmaylov, J.B.A.F., Zheng, G.,
494 Sonnenberg, J.L., Hada, M., Ehara, K.T.M., Fukuda, R., Hasegawa, J., Ishida,
495 M., Nakajima, T., Honda, O.K.Y., Nakai, H., Vreven, T., Montgomery, J.A. Jr.,
496 Peralta, F.O.J.E., Bearpark, M., Heyd, J.J., Brothers, E., Kudin, V.N.S.K.N.,
497 Kobayashi, R., Normand, J., Raghavachari, A.R.K., Burant, J.C., Iyengar, S.S.,
498 Tomasi, J., Cossi, N.R.M., Millam, J.M., Klene, M., Knox, J.E., Cross, J.B.,
499 Bakken, C.A.V., Jaramillo, J., Gomperts, R., Stratmann, R.E., Yazyev,
500 A .J.A .O., Cammi, R., Pomelli, C., Ochterski, J.W., Martin, K.M.R.L.,
501 Zakrzewski, V.G., Voth, G.A., Sal-vador, J.J.D.P., Dapprich, S., Daniels, A.D.,
502 Farkas, J.B.F.O., Ortiz, J.V., Cioslowski, J., Fox, D.J., Gaussian 09, Gaussian,
503 Inc, Wallingford, CT, 2009.
- 504 31. Islam, M.M., V.S. Bryantsev, and A.C.T. van Dian, *ReaxFF Reactive Force*
505 *Field Simulations on the Influence of Teflon on Electrolyte Decomposition*
506 *during Li/SWCNT Anode Discharge in Lithium-Sulfur Batteries*. Journal of the
507 Electrochemical Society, 2014. **161**(8): p. E3009-E3014.
508